SOLAR CELLS BASED ON a-$Si_{0.80}$ $Ge_{0.20}$:H AMORPHOUS FILMS

B.A. NAJAFOV

Institute of Radiation Problems, Nat. Acad. Sci. of Azerbaijan
(31a, H. Javid Ave., Baku Az -1143, Azerbaijan)

UDC 532

The electrical properties, spectral dependence of photoconductivity, ESR and IR absorption spectra of a- $Si_{0.80}$ $Ge_{0.20}$:H films, and a-$Si_{0.80}Ge_{0.20}$:H-based solar cell structures of the $p-i-n$ junction and Pt/ a-$Si_{0.80}Ge_{0.20}$:H Schottky-barrier types are examined. The results of studies show that the a-$Si_{1-x}Ge_x$:H ($x \leq 0.20$) material is thermodynamically stable and is important for manufacturing the solar energy converters. Solar cells with the energy conversion efficiency of 5.9 and 4.2% for $p-i-n$ and Pt/ a-$Si_{0.80}Ge_{0.20}$:H structures, respectively, have been obtained.

1. Introduction

At present, hydrogenated films of a-Si_{1-x}:H, a-$Si_{1-x}N_x$:H, a-$Si_{1-x}C_x$:H, a-$Ge_{1-x}C_x$:H, a-$Si_{1-x}O_x$:H, and a-$Si_{1-x}Ge_x$:H solid solutions are extensively studied. Amorphous silicon is gradually degraded by the exposure to light through the Staebler—Wronski effect and the hydrogen passivation, and the alloying with germanium can reduce (with the germanium content which does not exceed 20 mole%, $x \leq 0.20$) both the presence of high-density localized states in the energy gap and the film band gap itself and hence further improve the light absorption and stabilized efficiency [1—8]. At the same time, the investigations of the H—Si and H—Ge bond concentrations by ESR and IR absorption methods display that hydrogen passivating properties in a-Ge far worse than those in a-Si. Therefore, on a whole, the a-$Si_{0.80}Ge_{0.20}$:H film photoefficiency turns out to be somewhat lower than that of a-Si:H [5].

In this work, the electrical properties, spectral dependence of the photoconductivity, ESR and IR absorption spectra of a-$Si_{0.80}Ge_{0.20}$:H films and a-$Si_{0.80}Ge_{0.20}$:H-based solar cell structures of the $p-i-n$ junction and Pt/ a-$Si_{0.80}Ge_{0.20}$:H Schottky-barrier types are examined. Solar cells with energy conversion efficiencies of 5.9 and 4.2% for $p-i-n$ and Pt/ a-$Si_{0.80}Ge_{0.20}$: structures, respectively, in the 90 mW/cm^2-sunlight have been obtained.

2. Experiment

a-$Si_{0.80}Ge_{0.20}$:H thin films of 0.8μm in thickness were fabricated by the plasmochemical deposition method at a substrate temperature of 200 °C. The rate of deposition of the material on the substrate was 3 Å/s, and the distance between the target and the substrate $L \approx 25$ cm. The growing of a film was carried out for about 1 h. The electric field strength upon the measurements of the electrical properties of films did not exceed 10^4 V/cm. In the measurements of the temperature dependence of the electrical properties, an aluminum—chrome thermocouple was used. The thickness of the a-$Si_{0.80}Ge_{0.20}$:H films was determined by the optical method under conditions of a rise of transport phenomena. The hydrogen concentration in the films was calculated by the effusion method and with the use of absorption spectra, and its value amounted to 1.7÷17.3 at.%. The deposition process was executed at various partial pressures in a hydrogeneous plasmic medium that had been obtained by means of a permanent magnet, magnetron, and a RF field. $Si_{0.80}Ge_{0.20}$ crystalline alloy plates 60—63 mm in diameter served as a target. The amorphism of films was checked by electrographic methods. As a substrate, crystalline Si for IR (radio frequency) measurements and an aluminum foil for ESR (electron spin resonance) measurements were used. The ESR and IR measurements were performed with JEOL PE 3X and IR-29 spectrometers at a temperature of 80 K. Parameters of the ESR spectrum and the concentration of paramagnetic centers were determined by the M_n^{2+} pattern in the MgO lattice. Upon the film fabrication, the RF frequency was 230 MHz (a power was 50 W). The relative error upon the determination of the hydrogen concentration was 10—12 at.%. For thin-film solar cells in the visible range of the absorption spectrum, the condition $\alpha d \geq 1$ was valid, where d is the thickness of the active layer, and the absorption coefficient was $\alpha = 8 \times 10^4$ cm^{-1} for a-$Si_{0.80}Ge_{0.20}$:H films.

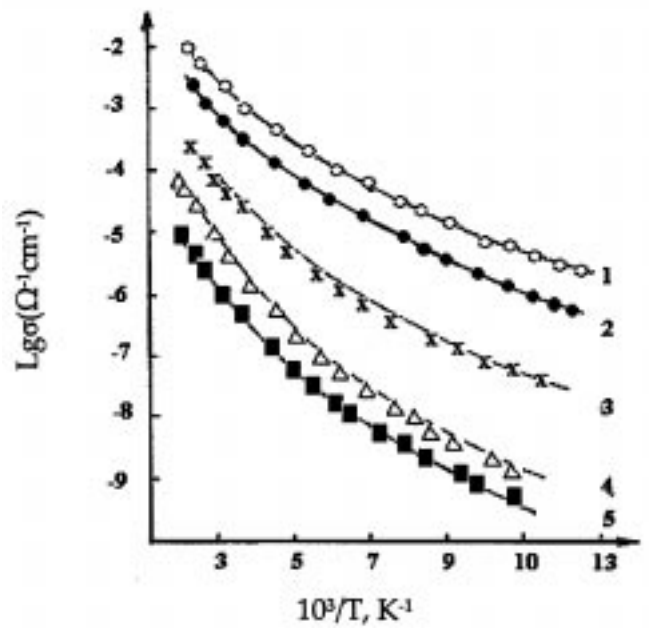

Fig. 1. Temperature dependence of the dark conductivity $\sigma(T)$ as a function of $1/T$ for a-$Si_{0.80}Ge_{0.20}$:H films ([H]=1.7 (*1*), 3.9 (*2*), 7.1 (*3*), 12.1 (*4*), 17.3 (*5*) at.%)

3. Results and Discussion

3.1. Electrical properties of the a-$Si_{0.80}Ge_{0.20}$:H solid solution thin films

The measurements showed that the conductivity $\sigma(T)$ as a function of temperature has two regions. Over the range 250—350 K, the conductivity is given by the formula

$$\sigma(T) = \sigma_0 \exp(-\Delta E/kT), \tag{1}$$

where σ_0 is the pre-exponential factor which varies within the limits of 8.91×10^{-2}—5.62×10^{-5} $\mathrm{Om^{-1}cm^{-1}}$ and is determined by the curve slope (Fig. 1). ΔE for electrons takes the form $\Delta E = E_C - E_\mathrm{F}$, where E_C and E_F are, respectively, energy levels in the conduction and valence bands. At $T \leq 250$ K, the conductivity is dictated by the hopping character, to which the linear relation $\lg(\sigma T^{1/2})$ against $T^{-1/4}$ testifies.

For low-temperature regions, the curves are fitted with the relation [9]

$$\sigma = \sigma_1/T^{1/2} \exp[-(T_0/T)^{1/4}], \tag{2}$$

where

$$\sigma_1 = e^2 a^2 \gamma_\mathrm{ph} N(\varepsilon_\mathrm{F}), \tag{3}$$

and

$$T_0 = (\lambda\alpha^3)/(kN(\varepsilon_\mathrm{F})). \tag{4}$$

Here, e is the electron charge, a is the interatomic distance (whose typical value equals 2 Å), γ_ph is the phonon frequency ($\sim10^{13}\mathrm{s}^{-1}$) at the Debye temperature, α is a parameter of the electron wave function damping in a localized state, α^{-1} is, accordingly, the radius of the localized wave functions of electrons (for the hydrogen concentration 1.7—17.3 at.%, its value equals 7—10.3 Å), λ is a dimensionless constant ($\sim$18.1), and $N(\varepsilon_\mathrm{F})$ is the state distribution near the Fermi level, $N(\varepsilon_\mathrm{F}) = 10^{19} \div 8\cdot10^{17}$ $\mathrm{cm^{-3}eV^{-1}}$. The $N(\varepsilon_\mathrm{F})$ parameter is determined by substituting the interatomic distance, a, in Eqs.(2) and (3) for the average length, R [10]. Then using a relation from [10, 11] at 100 K, the hopping length, R, can be computed with the formula

$$R = [9/8\pi\alpha N(\varepsilon_\mathrm{F})kT]^{1/4}. \tag{5}$$

Accordingly, for the hopping energy, E, one finds

$$E = 2/3\alpha RkT = (T_0/3\pi^{1/4})T^{3/4}. \tag{6}$$

This gives $R = 31.27 \div 51.46$ Å and $E = (0.029 \div 0.072)T^{3/4}$ eV.

The study of the films after the γ irradiation induced by a source with a radiation dose of 10^{17}—10^{18} $\mathrm{phot/cm^2}$ has shown that γ quanta passing through an a-$Si_{0.80}Ge_{0.20}$:H film do not produce new ruptured bonds.

3.2. Spectral dependence of the photoconductivity

The measurements of photoconductivity were performed in the photon energy range from 1.0 to 2.8 eV, and the optical excitation a halogen lamp with appropriate filters was used. Variations in the photocurrent over the range was computed by the formula [9, 12]

$$i_\mathrm{ph} = (eN_0\nu\tau/t_t)\exp(-\alpha d), \tag{7}$$

where N_0 is the number of photons per second, d is the film thickness, ν is the quantum yield, τ is the recombination lifetime, t_t is the transmission time of charge carriers, $t_t = d/E\mu_\mathrm{D} = d^2/V\mu_\mathrm{D}$, where μ_D is the drift mobility or the charge mobility under the effect of the E-field at room temperature, V is the applied voltage, and ν is the generation efficiency which is determined by the number of formed electron-hole pairs under the absorption of a photon (in the given case, $\nu \approx 1$). The recombination lifetime, τ, and the transmission time of charge carriers, t_t, were determined with the help of an electron oscillograph, respectively, by the rectangular and exponential parts of the current

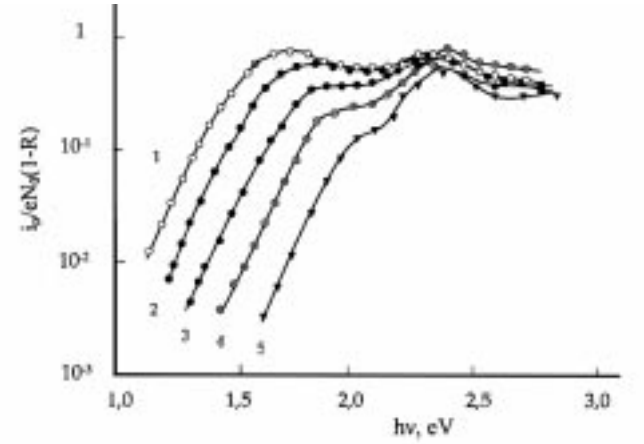

Fig. 2. Dependence of the photoconductivity on the photon energy in a-$Si_{0.80}Ge_{0.20}$:H films. Notations are the same as in Fig. 1

signal arising after the illumination of a film with a light pulse. We have found that, with a change of the hydrogen concentration, [H], the parameter $\nu\mu\tau$ varies between 10^{-7} and 10^{-5} $cm^{-2}B^{-1}$. The optical absorption coefficient, α, in all films was as great as 8×10^4 cm^{-1}.

On the basis of the data derived, it is presupposed that the photocurrent over the photon energy range from 1.0 to 2.8 eV linearly depends on the light intensity, and the particle recombination occurs from deeper recombination centers and obeys the law

$$i_{\rm ph} = AF^{\gamma}, \qquad (8)$$

where γ=0.9 [9]. The photon flux density F at all wavelengths was equal to 5×10^{12} $cm^{-2}s^{-1}$. To determine A, we used the weak-absorption spectrum regions, where the product $\nu\tau\mu_{\rm D}$ is independent of the photon energy. For specimens with the photon energy of 2.3—2.8 eV in the weak-absorption spectrum region, it may be assumed that $i_{\rm ph}/eN_0(1-R) \approx \alpha d\nu\tau/t_t$.

The electron transport in the films is given by the field effect method by the Spear model [9]. Fig. 2 presents the dependence of photoresponses of the film at room temperature as a function of the photon energy at different hydrogen concentrations.

It is seen from Fig. 2 that the electron generation efficiency does not change with a change in the hydrogen concentration. Hence, the quantum yields, ν, remain constant in the films fabricated by the indicated method at the hydrogen concentration from 1.7 to 17.3 at.%. It is also seen that, near the photon energy of 2.3 eV, all curves intersect each other and approximate 1 with a rise in the photon energy, which is connected with a rise in the electron generation efficiency in the material.

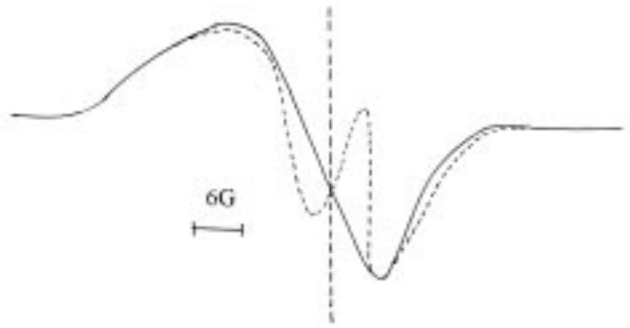

Fig. 3. ESR spectra taken at 80 K on a- $Si_{0.80}Ge_{0.20}$:H films ([H]=17.3 at.%)

Depending on the hydrogen concentration the border of photoconductivity is located within the photon energy limits from 1 to 1.5 eV, and the displacement of the border is associated with increasing of the gap width, $E_c - E_v$, and the Fermi level excitation (that displaces as the H concentration changes).

The plateau in Fig. 2 for all studied specimens over the photon energy range from 1.6 to 2.1 eV is interpreted as a consequence of the maximum of the density of states, E_y, and the posterior growth of the photoconductivity is due to transitions from one band to another one.

On the basis of these results, we may assert that γ stays constant with a change of the hydrogen concentration.

3.3. ESR and IR absorption spectra of a-$Si_{0.80}Ge_{0.20}$:H solid solution films

The ESR spectra of a-$Si_{0.80}Ge_{0.20}$:H (with [H]=17 at.%) at 80 K were asymmetric in form, inasmuch as they were composed of two components corresponding to the dangling bonds of Si and Ge, respectively (Fig. 3). At the same time, the observed signal was not a simple superposition of two signals (for Si and for Ge), since they violently interacted with each other and the resulting signal in the intervening interval aimed to take the form of a single line. For this reason, the observed spectrum on its left and on its right can be depicted as a superposition of two signals: one signal with the g factor equal to 2.004—2.006 and the linewidth of 51—65 G and the second one with the g factor equal to 2.018—2.022 and the linewidth of 73—86 G relating to the silicon and germanium dangling bonds, respectively. In this way, we can evaluate the densities of Si and Ge dagling bonds

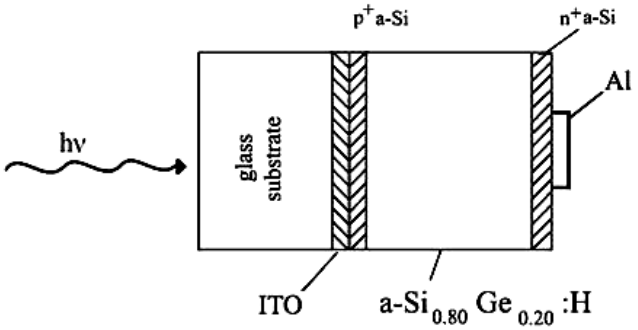

Fig. 4. Schematic diagram of the $p-i-n$ junction solar cell structure on the base of a-$Si_{0.80}Ge_{0.20}$:H ([H]=17.3 at.%)

taken separately. But, in accordance with the computation of molecular orbitals in a-$Si_{1-x}Ge_x$:H, the presence of atoms adjacent to the orbitals almost does not alter the g-value of ESR-signals from both Si and Ge dangling bonds [8]. By analyzing the IR absorption spectrum determined by the numbers of Si—H and Ge—H bonds, we found that the number of the dangling bonds of Ge is 8—10 times larger than that of Si [10]. It is proved that H atoms in a-$Si_{1-x}Ge_x$:H films are mainly bound to Si atoms. This fact is also confirmed by ESR investigations. The ESR investigations in a-Si_{1-x} Ge_x:H amorphous films with x=10 at.% Si ([H]=23 at.%) fabricated by the vacuum evaporation and the plasmochemical deposition have shown that the band gap set up by strongly localized centers is of the order of $10^{20} \div 10^{19}$ $cm^{-3}eV^{-1}$ [11, 13]. The localized centers are paramagnetic, and they define probably the dependence of electrophysical properties of the material, $\sigma(T)$ vs. $T^{-1/4}$, in the low-temperature range. Hence, in a-$Si_{0,80}Ge_{0,20}$:H films, we can find the paramagnetic center concentration

$$N_s = \alpha N(\varepsilon_F)kT \tag{9}$$

by the signal intensity, which gives unambiguously a value of the density of states provided that the effective energy of correlation between two electrons in the band gap, U, is much less than kT ($U \ll kT$), $N(\varepsilon_F)$ is the density of states near the Fermi level of the order of 10^{16} $cm^{-3}eV^{-1}$, and $\alpha \approx 3$ [14]. In case of $U \gg kT$, states lying below ε_F in U magnitude are paramagnetic independent of temperature. The study of the influence of γ-radiation on properties of amorphous hydrogenated a-$Si_{0.80}Ge_{0.20}$:H enables one to get the valuable information on defects in the material. Under γ-irradiation from a source with a radiation dose of 10^{17}—10^{18} photon/cm^2, the investigation has revealed that quanta do not produce torn bonds by passing through the a-$Si_{0.80}$ $Ge_{0.20}$:H film (as it would occur, e.g., under the irradiation by visible light).

3.4. Solar cells on the basis of a-$Si_{0.80}Ge_{0.20}$:H thin films

In this subsection, we consider some physical parameters of solar cells of Pt-barriers formed on a-$Si_{0.80}Ge_{0.20}$:H samples (with [H]=17.3 at.%) as well as the cell structure in its simplest form, a single sequence of $p-i-n$ layers. In order to obtain the galvanomagnetic effect, the film was illuminated by light of a power of ~90 mW·cm^2. For utilizing the $p-i-n$ structure, we chose a glass substrate and the ITO coating of about 500 Å in thickness which transmitted up to 80% of light. The i-layer was undoped, and the optical absorption coefficient, α, reached the value of $8 \cdot 10^4 cm^{-1}$ in the visible region of the spectrum and satisfied the relation

$$\alpha h\omega = B(h\omega - E_g)^2, \tag{10}$$

where B was determined by extrapolation of the dependence $(\alpha h\omega)^{1/2}$ on $h\omega$ and came to 539 $eV^{-1}cm^{-1/2}$, and E_g is the band gap width equal to 1.72 eV. The value of $\mu\tau$ for the i-layer amounted to 10^{-7} cm^2B^{-1}. In the given case, the generation efficiency $\nu \approx 1$. Thin p^+ and n^+ layers were 200—350 Å in thickness and produced in the discharge of SiH_4 having contained ~1% of B_2H_6 and PH_3 (Fig. 4). The doping levels of B_2H_6/ SiH_4 and PH_3/ SiH_4 were $\leq 10^{-4}$. Since the resistivity of doped a-Si:H was $\geq 10^2$ Ohm·cm, the ITO semitransparent conductive layer was used as a contact electrode on the illumined side of the cell. Furthermore, an Al layer was applied on the cell reverse side. In this case, the maximal efficiency was as high as 5.9%, and the largest values of the short-circuit current j_{sc}, open-circuit voltage V_∞, and the curve fill factor ξ were equal to 12.4 mA·cm^2, 790 mV, 0.55, respectively. Making use of the dependence j_{sc} on V_∞ from the expression

$$V_\infty = n'kT/q \cdot \ln(j_{sc}/j_0 + 1), \tag{11}$$

we determined the diode quality factor n' to be 1.6 under illumination.

In a similar manner, solar cells of the Pt/ a-$Si_{0.80}Ge_{0.20}$:H type were fabricated. A stainless steel was chosen as the substrate, and the ZrO_2 coating with the light transmittance of ~80% was used. In order to improve the performance over time and run of the cell, we deposited a thin 200-Å n^+ layer, which was produced from SiH_4, on the substrate (Fig. 5). The parameters of

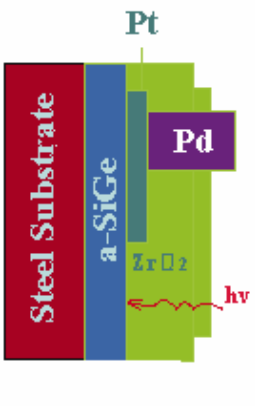

Fig. 5. Schematic diagram of the solar cell structure of the Pt/a-$Si_{0.80}Ge_{0.20}$:H ([H]=17.3 at.%) of the Schottky barrier type

the active layer have been considered above. Using the dark voltage-currwent characteristics, the saturation current density is defined as [14]

$$j_0 = q\mu_c N_c E_s \exp(-\varphi_B/kT), \tag{12}$$

where μ_c is the electron mobility in the conduction band, from which one deduces the dependence $\sigma(T)$ on $1/T$, and equals 6 $cm^2/(V{\cdot}s)$, N_S is the effective density of states in the conduction band (its value, 10^{21} cm^{-3}, was taken from [11]), and $E_s = 10^4$ V/cm. Knowing the experimental value for $j_0 = 10^{-10}$ A/cm^2, we determined the barrier height $\varphi_B = 1.2$ eV and the diode quality factor $n' = 1.4$ from the above-presented relation. From the capacitance-voltage ($C-V$) characteristics, we got 0.42 for the internal potential value and $\sim 3\cdot 10^{17}$ cm^{-3} for the charge spatial density. Then, using the relation [14]

$$W_B = (\varepsilon/2\pi q)^{1/2}(V_0/N)^{1/2} \tag{13}$$

for the impoverished region width, we got $W_B = 0.35$ μm. In Fig. 6, we present the current-voltage ($I-V$) characteristics (curves *1* and *2*) for a solar cell with the Pt/ a-$Si_{0.80}Ge_{0.20}$:H and $p-i-n$ structures after the illumination by a 90-mW/cm^2 light source. Using the dependence j_{sc} on V_∞, we got the diode quality factor n' under illumination to be 1.52. From Fig. 6 (curve *1*), we determined that the maximal efficiency comes to 4.2%. We also got that the largest values of the short-circuit current, j_{sc}, open-circuit voltage, V_∞, and the curve fill factor, ξ, were equal to 11.2 mA/cm^2, 650 mV, and 0.52, respectively. Fig. 7 presents the dependence of the collection efficiency on a wavelength of light with the falling photon flow of $10^{13} \div 10^{14}$ cm^2s^{-1} in the short-circuit regime, computed by the data on the optical

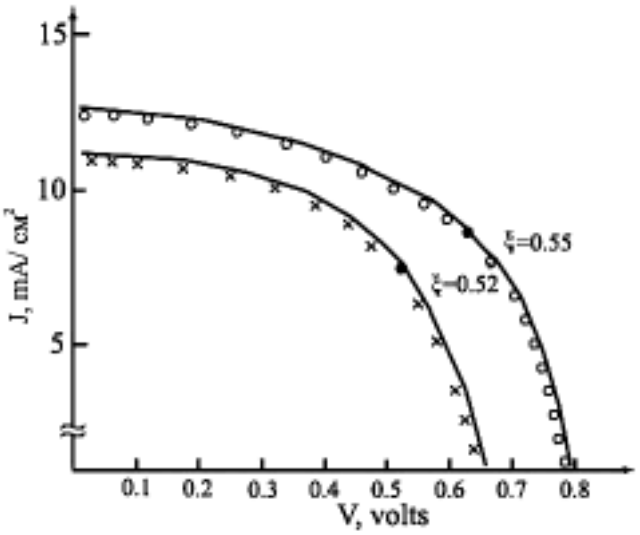

Fig. 6. $I-V$ characteristics for the solar cells under lightening with P=90 mW/cm^2 of the Schottky barrier type (*1*) and $p-i-n$ structure (*2*)

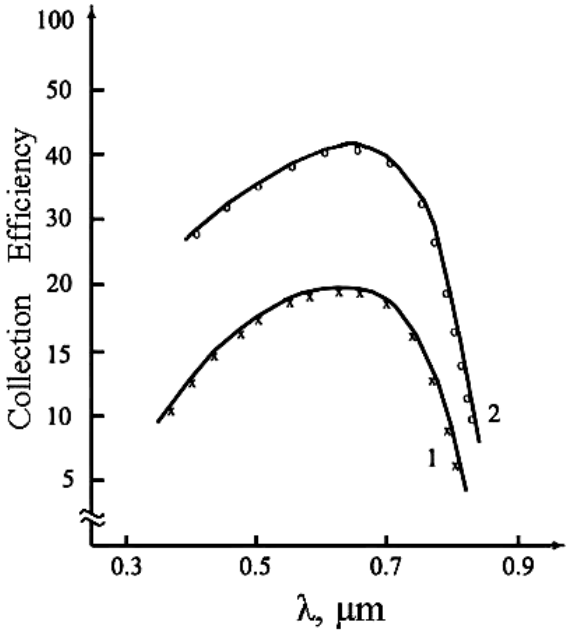

Fig. 7. Dependence of the collection coefficient on a wave length of light for the solar cells of the Schottky barrier type (*1*) and $p-i-n$ structure (*2*)

absorption for a film 0.5 μm in thickness. When computed, the photon flow is diminished by 80% to accommodate the limited optical transmittance of the

metallic film (curve *1*). In the same way, the collection efficiency for the $p-i-n$ structure is shown as curve *2*.

In the case of the photocurrent saturation, when all carriers excited by light are collected in the short-circuit regime, the measured collection efficiency does not depend on the reverse displacement of the voltage. A maximum of the collection efficiency corresponds to the wavelength $\lambda \leq 0.7$ μm. A decrease of the collection efficiency in the large wavelength range is explained, in general, by the absorption coefficient reduction for the active i-layer.

4. Conclusions

The results of the carried out studies makes it possible to assert that the a-$Si_{0.80}Ge_{0.20}$:H material is thermodynamically stable and is of importance for manufacturing the solar energy converters.

The obtained results allow us to assert that, for manufacturing the solar cells on the base of a-$Si_{0.80}Ge_{0.20}$:H, we can use thin films with a minimum concentration of paramagnetic centers N_S, the maximum hopping activation energy and the efficiency of the generation of electron-hole pair carriers, $\nu \approx 1$, and with the optical absorption coefficient α in the visible region of the spectrum. It has been shown that the solar cells with the largest short-circuit photocurrent density, j_{sc}, open-circuit voltage, V_∞, and the curve fill factor in cells, ξ, possess the best properties.

We emphasize that, for improving the quality of solar cells, the development of new technological installations and a further modification of properties of the active i-layer should be realized, and new combinatorial approaches to the optimization of devices must be developed in order to reach the best compromise on the thermodynamical stability, manufacturing cost, service life, and conversion efficiency.

1. *Schropp R.E.I., Zeman M.* Amorphous and Microcrystalline Silicon Solar Cells: Modeling, Materials and Device Technology. — Dordrecht: Kluwer, 1998.
2. *Practical* Photovoltaics: Electricity from Solar Cells/ Ed. by R.J. Komp, J. Perlin. — Aatec, 2002.— P.197.
3. *Kuznetsov V.J., Zeman M., Vosteen L.L.A. et al.* // J. Appl. Phys.—1996.— **80**, N11.— P.6496—6504.
4. *Budaguan G., Sherchenkov A.A., Gorbulin G.L., Chernomordic V.D.*// Phys. Condens. Matter.—2001.— **13**, N6.— P.6615—6624.
5. *Sherchenkov A.A.*// Semiconductors.— 2003.— **37**, N7.— P.763—765.
6. *Horvath Zs. J., Serenyi M., Adam M. et al.* // Phys. status solidi (c).— 2003.— P.1066—1069.
7. *Rosales-Quintero P., Torres-Jacome A., Murphy-Arteaga R., Landa-Vazques M.*// Semicond. Sci. and Technol.— 2004.— **19**, N3.— P.366—372.
8. *Amorphous* Semiconductors. Technologies and Devices / Ed. by Y. Hamakava. — Amsterdam: North-Holland, 1983.
9. *The Physics* of Hydrogenated Amorphous Silicon : Electronic and Vibrational Properties / Ed. by J.D. Joannopoulos, G. Lucovsky. — Berlin: Springer, 1984.
10. *Lewis A.*// Phys. Rev. Lett.— 1972.— **29**, N23.— P.1555—1558.
11. *Nadzhafov B.A.*// Semiconductors.— 2000.— **34**, N11.— P.1330—1333.
12. *Najafov B.A.*// Ukr. Fiz. Zh. — 2000. — **45**.— P.1221—1224.
13. *Akiharu* Morimoto, Takashi Miura, Minoru Kumeda, Tatsuo Shimizu // Jpn. J. Appl. Phys.— 1981.— **20**, N11.— P. 833—836.
14. *Amorphous* Semiconductors / Ed. by M.H. Brodsky. — Berlin: Springer, 1990.

Received 17.06.04

ПЕРЕТВОРЮВАЧІ СОНЯЧНОЇ ЕНЕРГІЇ НА ОСНОВІ АМОРФНИХ ПЛІВОК a-$Si_{0,80}Ge_{0,20}$:H

Б.А. Наджафов

Р е з ю м е

Досліджено електричні властивості, спектральну залежність фотопровідності, ЕПР та ІЧ-спектри поглинання в плівках a-$Si_{0,80}Ge_{0,20}$:H, а також структури сонячних елементів на основі $p-i-n$-переходу та типу бар'єра Шотткі Pt/a-$Si_{0,80}Ge_{0,20}$:H. Здобуті результати свідчать, що плівки a-$Si_{1-x}G_x$:H з $x \leq 0,20$ є термодинамічно стабільними і радіаційно стійкими матеріалами для виготовлення сонячних елементів. Отримано сонячні елементи з коефіцієнтом корисної дії $\eta = 5,9$ та 4,2% для структур $p-i-n$ та типу бар'єра Шотткі Pt/a-$Si_{0,80}Ge_{0,20}$:H відповідно.